From skin mechanics to tactile neural coding: Predicting afferent neural dynamics during active touch and perception

Yuyang Wei, Francis P McGlone, Andrew G Marshall, Adarsh Makdani, Zhenmin Zou, Lei Ren * and Guowu Wei*

***Abstract*— First order cutaneous neurons allow object recognition, texture discrimination, and sensorimotor feedback. Their function is well-investigated under passive stimulation while their role during active touch or sensorimotor control is understudied. To understand how human perception and sensorimotor controlling strategy depend on cutaneous neural signals under active tactile exploration, the finite element (FE) hand and Izhikevich neural dynamic model were combined to predict the cutaneous neural dynamics and the resulting perception during a discrimination test. Using *in-vivo* microneurography generated single afferent recordings, 75% of the data was applied for the model optimization and another 25% was used for validation. By using this integrated numerical model, the predicted tactile neural signals of the single afferent fibers agreed well with the microneurography test results, achieving the out-of-sample values of 0.94 and 0.82 for slowly adapting type I (SAI) and fast adapting type I unit (FAI) respectively. Similar discriminating capability with the human subject was achieved based on this computational model. Comparable performance with the published numerical model on predicting the cutaneous neural response under passive stimuli was also presented, ensuring the potential applicability of this multi-level numerical model in studying the human tactile sensing mechanisms during active touch. The predicted population-level 1st order afferent neural signals under active touch suggest that different coding strategies might be applied to the afferent neural signals elicited from different cutaneous neurons simultaneously.**

***Index Terms*—Neurophysiological, skin mechanics, FE Human hand, neural coding, active touch.**

Yuyang Wei is with the Department of Mechanical, Aerospace and Civil Engineering, The University of Manchester, Manchester M13 9PL, UK

Francis P McGlone is with the School of Natural Sciences and Psychology, Liverpool John Moores University, Liverpool L3 5UX, UK

Andrew G Marshall is with the Institute of Aging and Chronic Disease, University of Liverpool, Liverpool, UK and also with the School of Natural Sciences and Psychology, Liverpool John Moores University, Liverpool L3 5UX, UK

Adarsh Makdani is with the School of Natural Sciences and Psychology, Liverpool John Moores University, Liverpool L3 5UX, UK

Zhenmin Zou is with the Department of Mechanical, Aerospace and Civil Engineering, The University of Manchester, Manchester M13 9PL, UK

Lei Ren is with the Department of Mechanical, Aerospace and Civil Engineering, The University of Manchester, Manchester M13 9PL, UK and also with the Key Laboratory of Bionic Engineering, Ministry of Education, Jilin University, China (e-mail: lei.ren@manchester.ac.uk)

Guowu Wei is with the School of Science, Engineering and Environment, University of Salford, Manchester M5 4WT, UK (email: g.wei@salford.ac.uk)

I. Introduction

Our ability to perceive and manipulate objects relies fundamentally on subclasses of primary mechanosensory neurons in the glabrous skin of the hand. They provide tactile feedback enabling our somatosensory system to inform the sensorimotor control loop and build the interface between the world and the somatosensory cortex. The closed-loop control allows us to voluntarily perceive and manipulate objects during active touch, acquiring the information based on perception. The typical case of sensorimotor control is the reflex caused between cutaneous mechanoreceptors and the efferent motor neuron modulating muscle forces [1, 2]. The external stimuli are encoded by cutaneous receptors as 1st order afferent neural signals and then transmitted to the spinal cord and higher central nervous system (CNS) for further processing and decoding [3].

Over the past decades, research has focused on capturing the single-fiber afferent signals from the peripheral neural system [4, 5] using the technique of microneurography, applying numerical models to understand the neural dynamics and the mechanoelectrical mechanisms of the cutaneous receptors under different stimulus conditions. Quantifying the relationships between the stimuli and the state of stress/strain at the site of mechanoreceptors. In 2003, Dandekar et al. showed that the strain energy density can be quantitatively related with the membrane current through the cutaneous receptor and then applied this for predicting neural dynamics [6]. Another study was conducted by delivering passive stimuli to the finite element (FE) model, strain energy density (SED) was extracted for evaluating the afferent neural signals and validated against the microneurography results [7]. Similar numerical models based on continuum mechanics have also been applied to simulate population-level afferent signals under passive stimulation using model parameters derived from afferent spiking data in monkey glabrous skin [8]. However, previous numerical models did not incorporate the lateral sliding, realistic skin contact mechanism, or the hyper-elastic material properties of soft tissues. Also, muscle actuated active touch was not integrated with the numerical model, only passive stimuli were simulated with the simplified FE finger-tip model [7, 9]. It has been shown that different skin mechanics and neural responses during active touch could be altered from those evoked by passive stimuli [10-12]. However, the neural dynamics under muscle-driven active touch are difficult to capture using microneurography since the subject needs to be restrained and have relaxed muscles since electromyography signals may mask the afferent signals [13]. Therefore, the neural response or the mechanoelectrical properties of cutaneous neurons under active touch still remains unknown [8, 14] warranting being explicitly studied through the muscle-driven FE hand model.

Tactile perception is based on the integrated and processed population-level afferent signals from 1st order low threshold mechanoreceptors (LTM) in the skin, relays in the dorsal column nuclei and then via the thalamus to the somatosensory cortex. Research has shown that the collection of the group responses from 1st order cutaneous neurons is critical for understanding the tactile neural coding and the sensorimotor mechanism [2, 14]. Therefore, the second step of neural coding after the 1st order cutaneous mechanoreceptors is to understand how perception depends on these population-level afferent dynamics [3], the external stimuli should be related to the final human percept across the intact afferent transduction path under the active touch. The relationship between perception and afferent dynamics has been studied using *in-vivo* neural microstimulation of single peripheral afferents and the somatosensory cortex in awake subjects. Electrical stimulation of single afferent fibers in awake humans through a microneurography recording electrode, a technique termed intra-neural microsimulation, first reported by Ochoa et al [15], indicating that activity in a single afferent fiber could be perceived with perceptual qualities that depend upon the afferent type. A series of *in-vivo* tests conducted by stimulating area 3b to study temporal coding mechanisms in non-human primates [16] showed that the frequency discrimination of the subjects may depend on temporal coding and is more general than rate coding. However, recording afferent dynamics from population-level afferent fibers is technically demanding, and the invasive experiment on living subjects cannot be avoided [17, 18]. Implementation of the numerical model might be an effective method to obtain the fairly accurate population-level cutaneous signals and study the coding mechanism across the intact somatosensory path from the external stimuli to the final perception. Also, this study presents the possibility of using FE based integrated numerical model as a novel method to investigate the human sensorimotor mechanisms.

II. METHODOLOGY

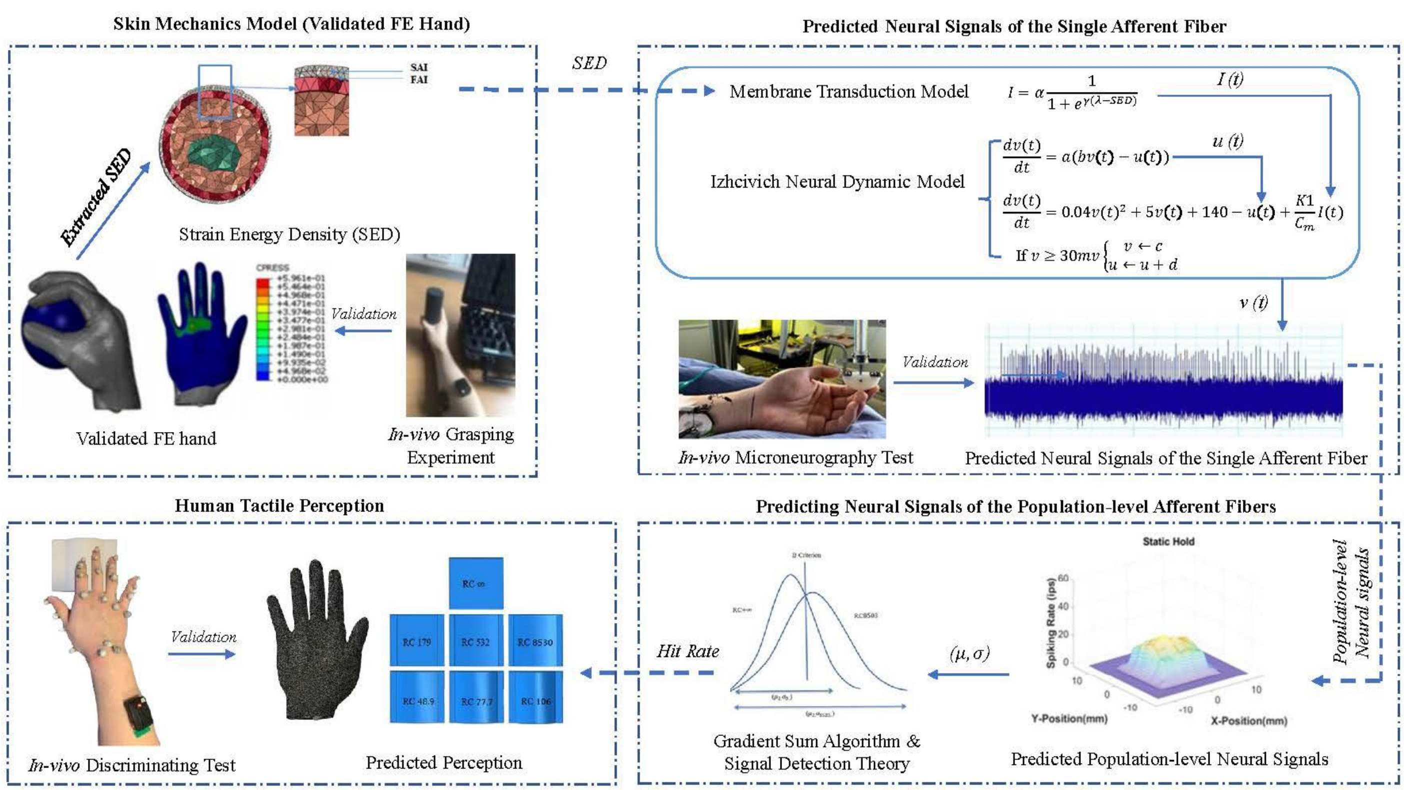

Fig. 1. Main procedure of this research. From the development of the FE human hand model to the predictions of the tactile neural signals. At the first step (Skin mechanics model), the SED during active touch was extracted at the site of mechanoreceptors as input of the membrane transduction model of step 2 (Predicting neural signals of the single afferent fiber). The neural signals from a single afferent tactile fiber were predicted and validated against microneurography results, this procedure was duplicated in step 3 (Predicting neural signals of the population-level afferent fibers) to derive the population-level afferent tactile neural signals. The signal detection theory was employed to correlate the computed neural signals with predicted human perception or the hit rate in step 4 (human tactile perception). The predicted hit rate was validated with the results of the *in-vivo* discrimination test.

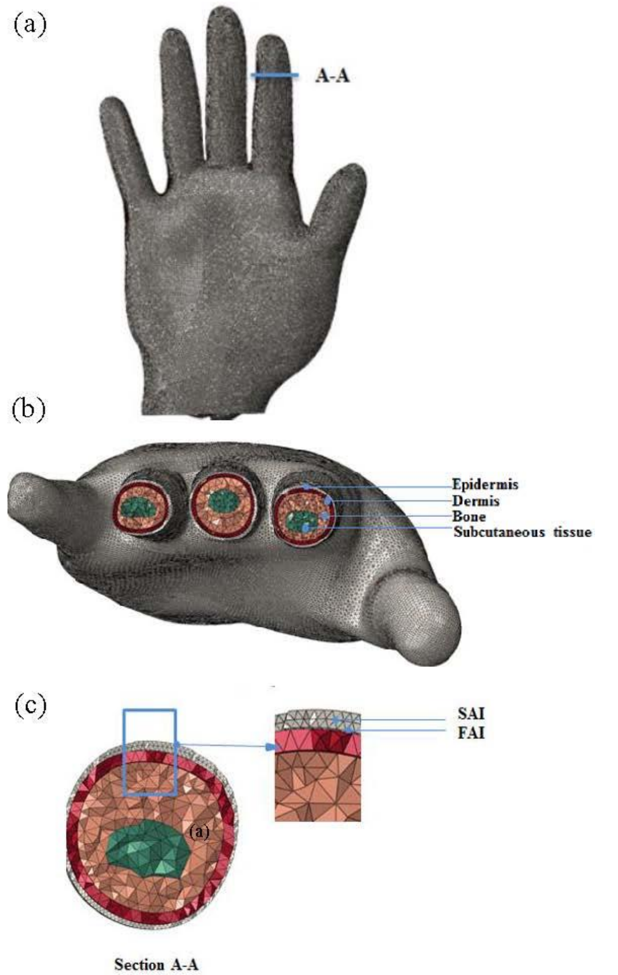

Fig. 2. The skin mechanics model (a). The FE human hand model. (b). The four-layered structure was modelled for extracting proper SED during the active touch including bones, subcutaneous tissue, dermis and epidermis from inside to outside. (c). The cross-sectional view of the index finger. The locations for extracting strain energy density of SAI/FAI mechanoreceptor. The SED of SAI was extracted at the top point of the tetrahedral element at the boundary between the epidermis and dermis while for FAI unit, the SED was computed at the bottom points of the elements on the epidermis-dermis boundary.

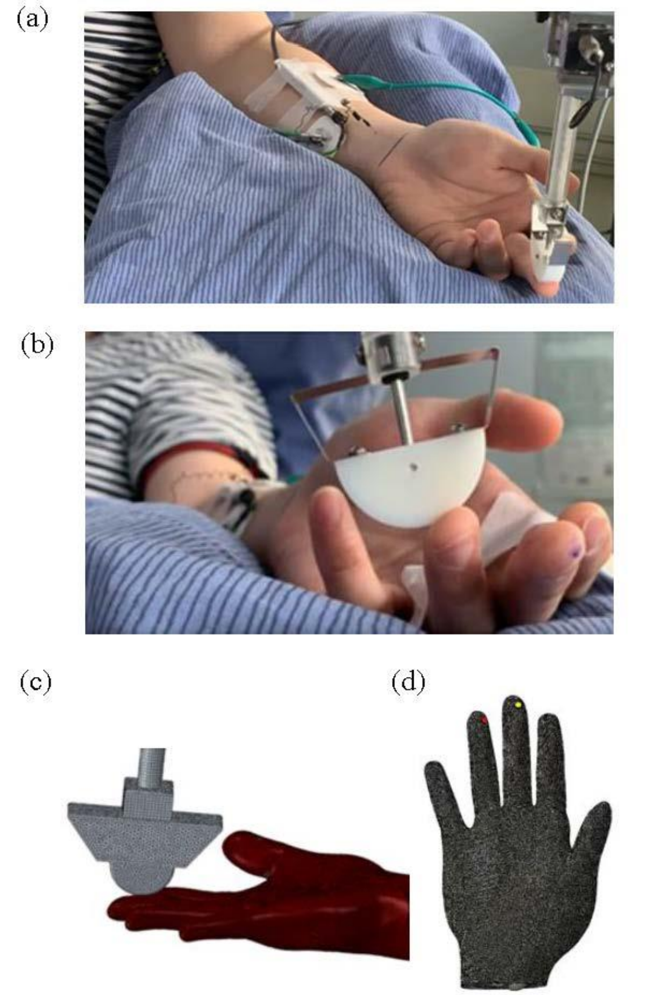

Fig. 3. The Microneurography test and the corresponding FE simulations. (a) Tungsten electrode (FHC Inc. Bowdoin, ME USA) was inserted into median nerve, capturing the single-afferent neural signals. (b). The Robotic Tactile Stimulator (RTS) (Dancer Design Inc. Merseyside, UK) was used to deliver the stimuli onto the receptive field of a tactile unit. The RTS delivered a sweeping motion across the receptive field of the tactile unit with a specified contact force. (c) The FE simulation of the experiment. (d) The locations of the SAI and FAI tactile unit captured during microneurography which are highlighted with yellow and red dot respectively on the FE hand.

The integrated numerical model was developed, optimized and validated on three different levels (see Fig. 1): A) Skin mechanics (strain/stress environment at the site of the cutaneous mechanoreceptors). B) To give the explicit transformation between skin mechanics and neural activity. (Predicted neural action potentials of a signal tactile fiber were optimized and validated against the results of microneurography). C) Population-level neural signals to human perception. (Predicted population-level tactile neural signals were compared with the *in-vivo* experimental results, signal detection theory was used to make the decision). This research began with finding the parameter to link the skin mechanics with the transduction membrane current across cutaneous neurons. The SED and other stress/strain values were compared with the experimental results of microneurography, and it was found that SED achieved the most accurate representation of cutaneous neuron dynamics. The neural signal of a single tactile afferent fiber was predicted as follows: The 3D FE human hand was used to simulate the procedure of active touch as skin mechanics model, the SED was chosen among the stress/strain related values and transferred into membrane current flowing over the mechanoreceptors by using the mechanoelectrical transduction model. The Izhikevich neural model was applied to generate the action potentials based on the predicted membrane current. The population-level afferent tactile signals were computed over the fingertips by duplicating the procedure of converting SED to neural dynamics for the single tactile afferent fiber. At the same time, the published numerical model 'TouchSim' [8] was employed as the benchmark to compute neural response under passive stimuli and compare with the performance of the multi-level numerical model developed in this research.

A. Skin mechanics model-FE human hand

A subject-specific FE human hand model [19] (see Fig. 2(a)) was developed to obtain the propagation of stress/strain during the procedure of active touch. The FE model includes the geometry of the epidermis, dermis,

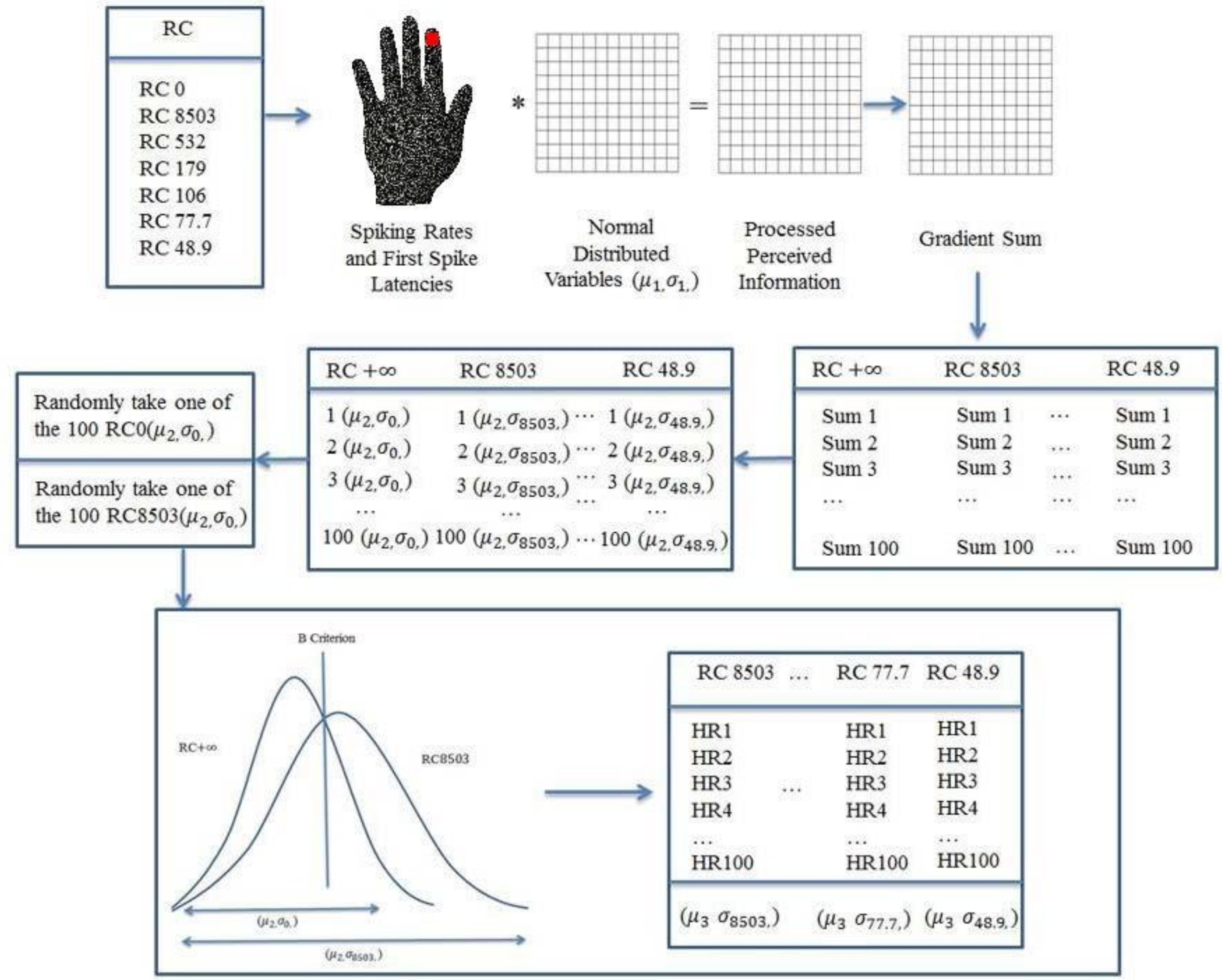

Fig. 4. The flow chart of the gradient sum approach for the population-level validation. Six convex with different radius were discriminated from the flat plate. First, the random noise is added through multiplying the neural action potential or the first spike latency of the tactile units by a pair of random variables with a mean value μ=1 and the standard deviation σ varied between 0.015 and 0.085. Second, the gradient sum of the elements is calculated by summing the gradients of all 100 elements together (100 SAI mechanoreceptors (elements) distributing over $1cm^2$ area on the finger pad. Third, the first and second steps are repeated 100 times for all the 6 convex resulting in 600 gradient sums totally,100 pairs of μ_2, σ_2 are derived for each convex. Fourthly, two pairs of (μ_2, σ_2) from the plate and convex were randomly selected. The signal detection theory (SDT) was used to judge whether the FE hand can differentiate the convex from the flat plate. This procedure is repeated for 100 times and the 100 discrimination accuracies or hit rates (HR) were computed for discriminating each convex surface.

subcutaneous tissue (see Fig. 2(b)), and the bones reconstructed based on the MR and CT images taken from a 23-year-old male subject. The material properties of soft tissues were defined as isotropic hyper-elastic, and the bones were assigned with the isotropic linear elastic material.

The mesh size of the epidermis and dermis was set to be 0.1mm, 0.7mm-mesh size was assigned for subcutaneous tissue and the bones. 1,002,915 C3D8H elements were meshed onto this FE hand model. Three grasping (cylinder grasping, spherical grasping, and precision gripping) were performed. The predicted results agreed well with the *in-vivo* experiment in terms of contact pressure and contact area and the relative differences between the two results are below 20%. The predicted contact area and contact pressure can provide the bulk mechanical response of the tissue layers [19, 20]. The detailed process for developing and validating the FE human hand can be found in our previous study [19]. Therefore, this FE human hand model is employed to produce the stress/strain related quantities as the skin mechanics model.

B. Predicting tactile signals of the single afferent neural fiber

1) The combined transduction and neural dynamic model for predicting cutaneous neural signals

The mechanoelectrical transduction function was firstly applied on the hair cell to explain the transducer adapting property [21]. Researchers also used these transduction functions to describe the mechanoelectrical transaction properties of the cutaneous mechanoreceptors and gained a good accuracy [7, 9, 22]. The SED at the site of the mechanoreceptor (see Fig. 2(c)) was extracted from the FE human hand and transformed to membrane current using the transduction function (equation 1). α, γ, λ are the

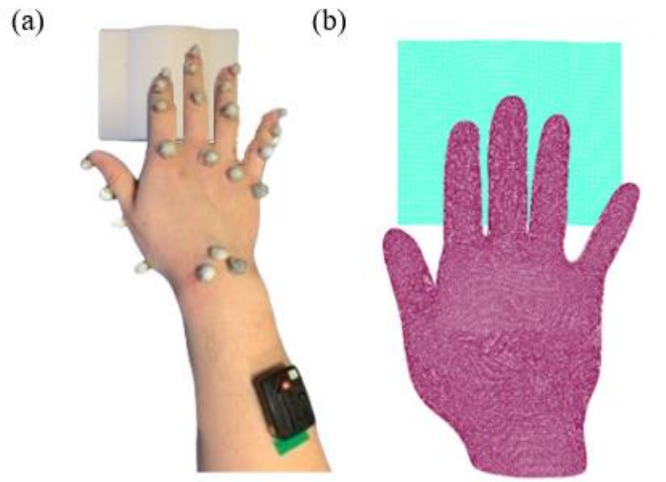

Fig. 5. *In-vivo* differentiation test and the corresponding simulation with the FE human hand (a). The *in-vivo* discrimination test. The subject was blind-folded and asked to differentiate two convex with different radius only through tactile perception. The markers were used to capture the hand kinematics during active touch using the Vicon System (Oxford Metrics Ltd., Bilston, UK). The Delsys Trigno (Delsys Inc., Boston, US) was applied to record EMG signal of the muscle. (b) The FE simulation of the discrimination test.

parameters determined through model fitting when the difference between predicted values and results of microneurography test are minimized.

$$I(SED) = \alpha \frac{1}{1+e^{\gamma(\lambda - SED)}} \ldots\ldots\ldots\ldots\ldots\ldots\ldots (1)$$

The cutaneous LTMs found in the glabrous skin of the human hand have distal axons that branch in the skin with irregularly spaced transduction sites [23, 24]. The spatially complex and overlapped receptive fields of the cutaneous neurons and the distance between the interdigitating subfields might determine the limit of the spatial resolution of human [25]. For this multi-level numerical model, each cutaneous tactile neuron is assumed to branch into 16 sensory organs according to the literature [26-30], echoing the fact that the first-order tactile neurons innervate on the order of ten mechanoreceptors. To simulate the heterogeneous receptive fields with highly sensitive zones of the branched axons, the SED was randomly selected at the nodes in the circular area with a diameter of 3mm [31]. At the same time, the SED was also extracted from the evenly distributed nodes for comparison and evaluating the effects of the non-uniformly distributed receptive fields of cutaneous neurons on tactile performance as is shown in Fig. S1. The neural responses were then computed based on the SED extracted from these nodes under the two different distribution patterns.

To mimic the biological neural dynamics of the tactile mechanoreceptor, the Izhikevich neural dynamic model was applied [32]. This neural dynamic model has been found to be able to reproduce the spiking, bursting response and the adaptation properties of the cutaneous mechanoreceptors [9, 22]. Among the four major types of low-threshold mechanoreceptors in the human hand, the SAI and FAI units were modelled to investigate the human sensing mechanism during spatial discrimination or active exploration in this study. Because the responses of SAI and FAI are critical to detailed feature discrimination [30, 33, 34] and sensorimotor control [35] which enables the explorative role of the hand. The responses of SAII and FAII units play a minor role in feature discrimination [34] which were not included in this numerical model.

The dynamic of the membrane potentials of SAI and FAI are defined as follows:

$$\text{SAI: } \frac{dv(t)}{dt} = 0.04v(t)^2 + 5v(t) + 140 - u(t) + \frac{K1}{C_m} I(t) \quad (2)$$

$$\frac{du(t)}{dt} = a(bv(t) - u(t)) \ldots\ldots\ldots\ldots\ldots\ldots (3)$$

$$\text{FAI: } \frac{dv(t)}{dt} = 0.04v(t)^2 + 5v(t) + 140 - u(t) + \frac{K2}{C_m} \frac{dI(t)}{dt} \quad (4)$$

$$\frac{du(t)}{dt} = a(bv(t) - u(t)) \ldots\ldots\ldots\ldots\ldots\ldots (5)$$

The auxiliary function is defined as followed:

$$\text{If } v \geq 30mv \begin{cases} v \leftarrow c \\ u \leftarrow u + d \end{cases} \ldots\ldots\ldots\ldots\ldots\ldots (6)$$

Where a,b,c,d are neuron parameters, u is the membrane recovery variable , v is the membrane potential.

2) In-vivo microneurography test

The subject gave informed consent to participate in the microneurography recording, which was approved by the Liverpool John Moores University Research Ethics Committee.

To optimize and validate the predicted afferent neural signals, microneurography was carried out. We have found that the spiking features and the selective response property of the same type of tactile units located at fingertips are similar to each other according to our microneurography results and the literature [36-38]. Therefore, the response of a single SAI/FAI tactile unit was recorded and used for developing the integrated numerical model. The same subject involved in developing the FE hand was recruited again for microneurography. The subject was required to lie on a medical chair with the forearm restrained. A tungsten microelectrode (FHC Inc. Bowdoin, US) was inserted into the skin at the wrist and electrical stimulation was delivered through the electrode to roughly determine its position in relation to the median nerve (see Fig. 3(a)). After locating and entering the nerve, the electrode was adjusted manually to search for tactile units. The action potentials were amplified and visualized by Neuro Amp EX and physiological data analysis software LabChart (ADInstruments Ltd. Oxford, UK) respectively. The receptive field was stimulated by the rotatory tactile stimulator (RTS) (Dancer Design Inc. Merseyside, UK) with varying forces (ranging from 0.2 to 2.4N with an increment of 0.2N). The stimulator delivered a ‘sweep’ stimulus onto the marked receptive field of the afferent tactile fiber as are shown in Figure 3(b) and the corresponding FE simulation is presented in Figure 3(c). The locations of the SAI (yellow dot) and FAI (red dot) tactile units captured during microneurography are shown in Figure 3(d). The spiking rates were derived for each second, resulting in 121 data points for the SAI unit under five stimulating forces (0.6, 1.0, 1.4, 1.8, 2.4N) while 131 data points were obtained for the FAI unit under six stimulating forces (0.4, 0.8, 1.2, 1.6, 2.0, 2.4N). The firing rate was calculated by taking the average of the reciprocal inter-spike intervals (ISI):

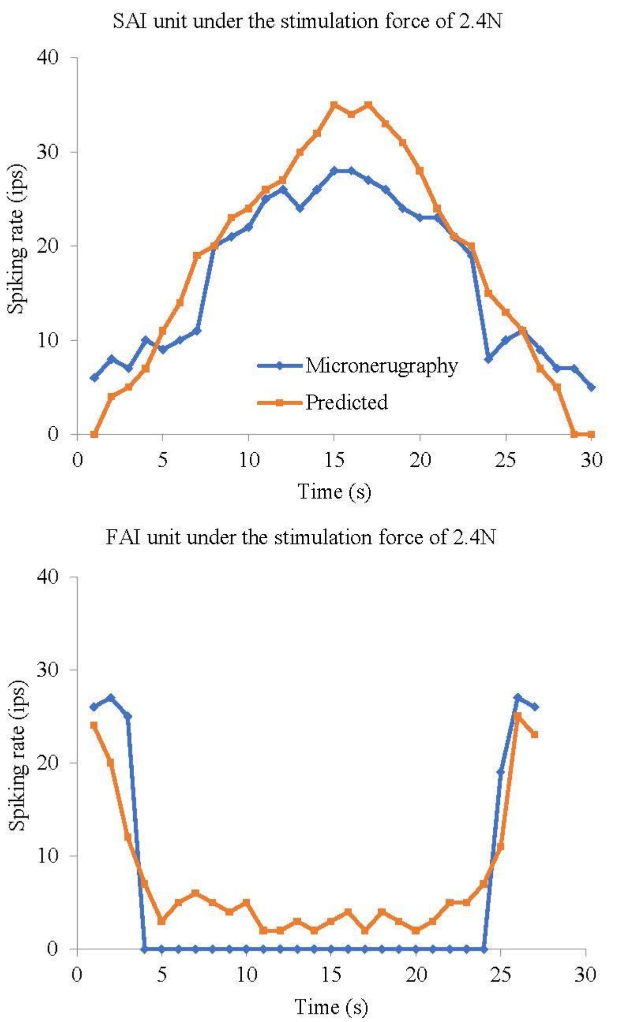

Fig. 6. The validation results for the single SAI and FAI tactile fiber. The predicted neural signals of SAI and FAI unit were compared with the results of microneurography.

$$ISI_I = t_i - t_{i-1} \ldots\ldots\ldots\ldots\ldots\ldots\ldots\ldots\ldots\ldots (7)$$

$$ISI_i = \frac{1}{a-b}\sum_{i=b}^{a} ISI_i \ldots\ldots\ldots\ldots\ldots\ldots\ldots\ldots\ldots (8)$$

$$f = \frac{1}{ISI_d} \ldots\ldots\ldots\ldots\ldots\ldots\ldots\ldots\ldots\ldots\ldots (9)$$

Where a-b= the number of ISIs.

3) Parameter optimization and validation for transduction and neural dynamic model based on the subject-specific microneurography data

The membrane current transduction and neural dynamic model were optimized against the results of the microneurography data by using the response surface method (RSM). Seven parameters in this integrated model were optimized against experimental results. Similar cross validation algorithm has been applied by other researchers to fit the parameters of neural dynamic model with experimental results [7].

The action potential signals under the stimulating force of 2.4N for SAI and FAI unit were separated for the validation (out-of-sample validation) while the rest of the data (Stimulating forces of 0.6, 1.0, 1.4 and 1.8N for SAI and 0.4, 0.8, 1.2, 1.6, 2.0 for FAI unit) were used to fit the computational model by using the RSM algorithm. The seven parameters:α, γ, λ of the transduction model and a, b, c, d of the Izhikevich model were optimized. The RSM algorithm aims to derive the specific combinations of these parameters which produce the best goodness of fit. (The fractional sum of squares (FSS, see equation 10.) between our subject-specific microneurography data and the predictions were minimized).

$$FSS = 1 - \frac{\sum_{i=1}^{n}[(exp)_i-(pre)_i]^2}{\sum_{i=1}^{n}{(exp)_i}^2} \ldots\ldots\ldots\ldots\ldots\ldots (10)$$

Where the exp stands for the microneurography test result, pre is the predictive result, n is the number of the data points.

The initial parameters values are $\alpha = 2.46 \times 10^{-5}$ mA, $\gamma = 0.0046\,Pa^{-1}$, $\lambda = 506.74Pa$, a = 0.02 Ohm, b = 0.2, c = -65mv, d = 6mv, these values are obtained from the literature [9, 39]. The procedure of parameter optimization was carried out in 4 steps. (a) Firstly, all the seven parameters were coded with specific increments less than two orders of magnitude of the initial values. (b) Secondly, all the parameters were increased or decreased for one increment and the FSS was derived for each trial resulting in totally 2^7 combinations. (c) Thirdly, the relationship between the optimized parameters and the FSSs was obtained through linear regression. (d) Fourthly, the magnitude and direction in which to optimize the parameters were determined by the combinations of the variation resulting in the largest increment of FSS. (e) Step (d) was repeated several times until the FSS was no longer increased. This optimizing procedure was conducted in Design Expert (Stat-Ease, Inc. US). After optimizing the parameters by using the RSM algorithm, the predicted neural signals of the integrated model achieved a good agreement with the results of microneurography in this study.

C. Predicting tactile signals of the population-level afferent neural fiber and its perception

1) The gradient sum algorithm and signal detection theory for relating the population-level neural activities with human perception

The psychophysical prediction is made by simulating the procedure of active touch during the discrimination test. The active touch was divided into two different procedures: 'dynamic ramp-up' and 'static hold', the former stands for the onset of the contact with an increased fingertip contact force and the latter represents the procedure of the stable contact with the object. The FE hand model was configured in a population density of 100 and 144 receptors/cm^2 for SAI and FAI units within the contact area of $1cm^2$ on the fingertip, discriminating the convex surfaces with different radius of curvature (RC) ranging from RC8530mm to RC48.9mm. Active touch was simulated by using the FE hand with the muscle forces and kinematics captured during the *in-vivo* discriminating experiment. The neural activities of the afferent tactile fibers within the contact area were computed and the Gradient Sum method [7] was used to correlate the FE hand's population-level neural dynamic signals with the discrimination accuracy or the tactile perception. The Gradient Sum method transmits the parameters between receptors and derives the gradients of spiking rates or first

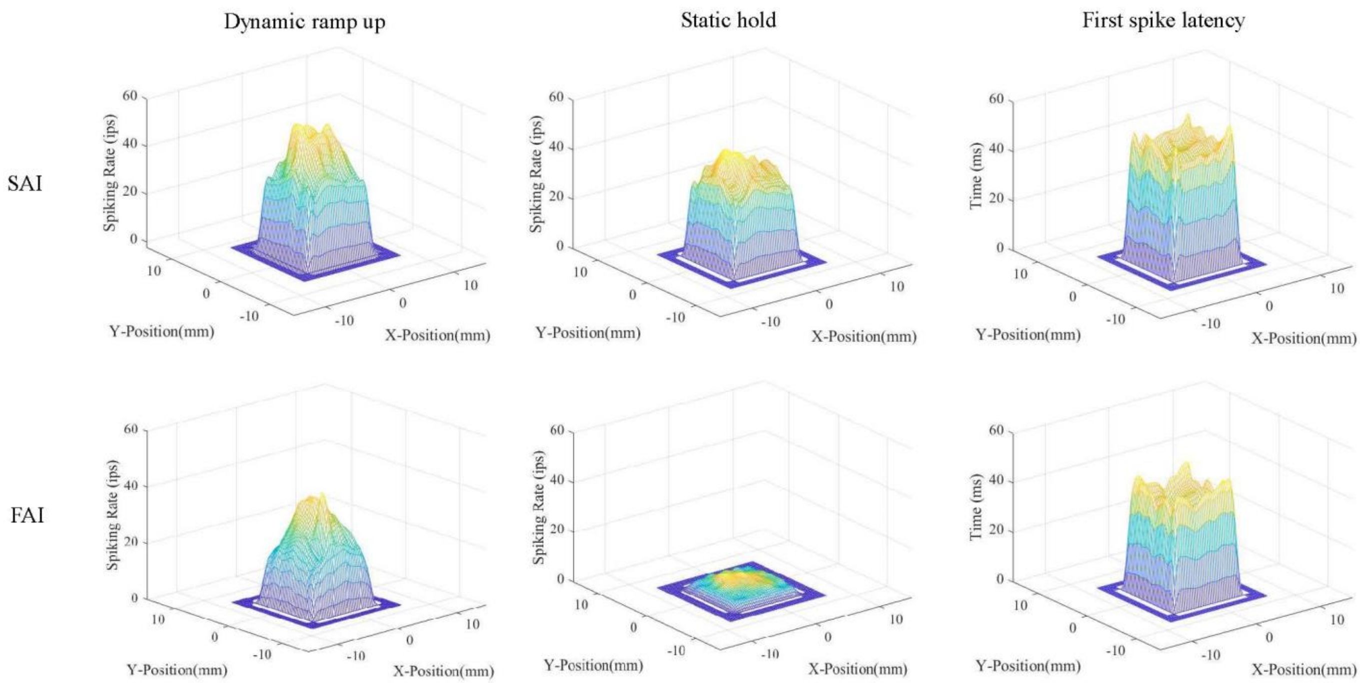

Fig. 7. Predicted neural activities of population-level SAI (first row) and FAI (second row) tactile units on index fingertip under the contact with the convex surface of RC77.7 mm. The horizontal axis stands for the locations of mechanoreceptors within the areas for extracting the SED, the vertical axis is the spiking rate or first spike latency. The active touch was divided into two separate stages including the ‘dynamic ramp-up’ and ’static hold’.

spike latencies from adjacent elements. The procedure of predicting the population-level tactile neural spike is shown in Figure 4(a) First, random noises were added through multiplying neural action potential and first spike latency of all units in one convex surface by a pair of random variables (μ_1, σ_1) with mean valueμ_1=1 and the standard deviation σ varied between 0.015 and 0.085. (b) Second, the gradient sum of the elements is calculated by summing all the parameter gradients around one single element. 100 gradients were derived per convex surface since 100 SAI mechanoreceptors (element) distributing over $1cm^2$ area was configured for each finger. All the gradients were added as the gradient sum. (c) Third, steps (a) to (b) are repeated 100 times for all the 7 convex surfaces resulting in 700 gradient sums totally, each time multiplying a new pair of (μ_1, σ_1). The corresponding 100 pairs of (μ_2, σ_2) are derived for each convex. (d) The signal detection theory (SDT) was used to judge whether the FE hand can differentiate the convex surface from the flat plate. For example, two pairs of (μ_2, σ_2) are randomly selected from RC8503mm convex surface and the flat plate as the inputs to SDT with the β=0.5. Therefore, the hit rate (HR) of convex surface RC8503mm is obtained. This procedure is repeated for 100 times to derive the 100 HR for discriminating convex surface RC8503mm. The hit rates were calculated as below:

$$d' = \frac{\mu_s - \mu_n}{\sigma} \ldots\ldots\ldots\ldots\ldots\ldots\ldots \text{(11)}$$

$$d' = \Phi^{-1}(H) - \Phi^{-1}(F) \ldots\ldots\ldots\ldots\ldots\ldots\ldots \text{(12)}$$

$$\ln(\beta) = \frac{[\Phi^{-1}(F)]^2 - [\Phi^{-1}(H)]^2}{2} \ldots\ldots\ldots\ldots\ldots\ldots\ldots \text{(13)}$$

d' is the distance between the means of the signal and noise in standard deviation unites. μ_s and μ_n are the mean values of the signal and noise, σ stands for the standard deviation of the noise. β is the criterion value and $\Phi^{-1}$is the inverse ‘Phi’ function of the Z distribution, the detailed information and calculation related to SDT can be found in [40].

(e) Finally, the step (d) is repeated for the other 5 convex surface and generates 500 HR. The (μ_3, σ_3) for each 100 HR of all the 6 convex surfaces are calculated. The procedure of predicting population-level neural signals of FAI units is the same with SAI.

2) In-vivo discrimination test

A psychophysical test of convex surface differentiation was performed to validate the predicted population-level afferent signals and study the neural coding mechanisms under the active touch. The *in-vivo* discrimination test was performed based on Goodwin’s research to determine the discrimination ability of humans [41].

To perform the discrimination test of population-level validation of SAI afferents, six convex surfaces with radius of RC8503, RC532, RC179, RC106, RC77.7, RC48.9mm and a flat plate (RC∞) were 3D printed. The same subject of the FE human hand model was recruited for the discrimination test. The capability of the subject to discriminate surfaces during the procedure of active touch was evaluated with 6 comparisons between different convex surfaces and the flat plates conducted. The subject was blindfolded and asked to sit at a table where the convex surfaces were presented in pairs, either with the same or different radius. The subject was required to judge whether the convex surfaces were the same or not. Only the fingertip of the index was allowed to touch the convex surfaces and the finger was restricted from

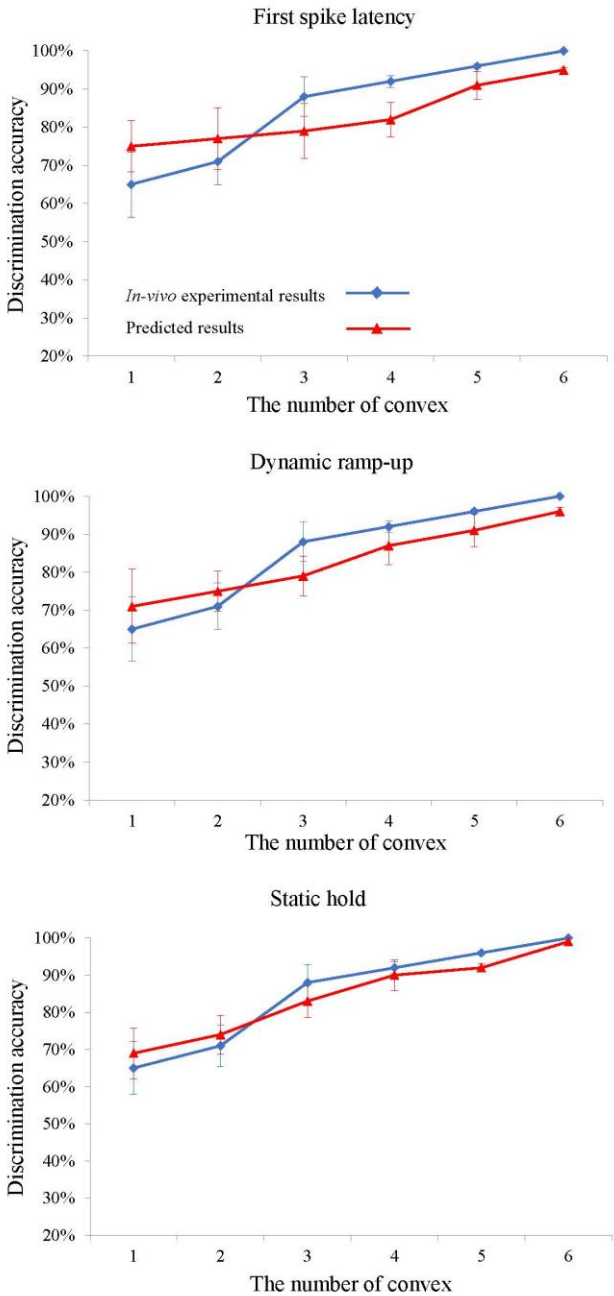

Fig. 8. The validation results of the population-level SAI tactile fibers. The predicted discrimination accuracy based on the afferent neural signals of SAI units were compared with the results of the *in-vivo* discrimination experiment.

adduction/abduction. The vertical distance between the peak of the convex surfaces and the index fingertip was kept the same, ensuring similar finger kinematics during touching different convex to avoid the effect of the proprioceptors located at finger joints. The test was carried out in blocks, each block contained 12 comparisons (6 pairs of flat-flat plate and 6 pairs of flat-convex, all convex surfaces were presented in each session), and the pair of surfaces varied randomly from block to block. In total, 30 blocks were performed, and the probability of detection was calculated for each convex surface, the whole test was repeated 6 times to achieve generality. Before the test, a few practice blocks were performed to train the subjects and ensure the reliability of the experimental results.

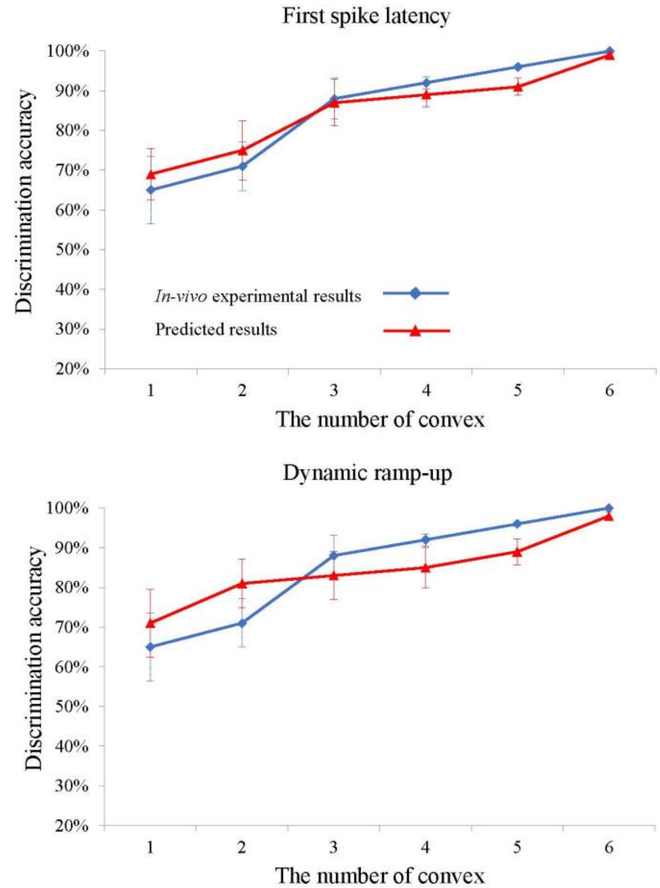

Fig. 9. The validation results of the population-level FAI tactile fibers. The predicted discrimination accuracy based on the afferent neural signals of FAI units were compared with the results of the *in-vivo* discrimination experiment.

During the discrimination test, the hand kinematics and muscle forces were captured by using the Vicon system (Oxford Metrics Ltd., Bilston, UK) and Delsys EMG Trigno (Delsys Inc., Boston, US) respectively (see Fig. 5(a)). The muscle forces were estimated based on the electromyography (EMG) signals. Before the discrimination test, maximum voluntary contraction (MVC) tests were carried out for each muscle using a Jamar dynamometer. The recorded EMG data was band-pass filtered (20–400 Hz) with a Butterworth filter and then rectified. The muscle forces were computed based on the maximum voluntary contraction forces. It was assumed that a linear relationship between the EMG signal and muscle force for isometric muscle contracting. Similar methods have been used by other researchers to calculate muscle forces under isometric contract [42-44]. These kinematic data and muscle forces were applied onto the FE human hand to simulate the discriminating experiment and then made the prediction (see Fig. 5(b)). The active touch procedure was divided into two steps: dynamic ramp-up of the contact force and static hold (Static hold procedure is not included in FAI validation since it only responds to onset and offset of the stimulation).

The benchmark model ‘TouchSim’ [8] for predicting the cutaneous neural response was employed to compare with the performance of this multi-level numerical model. Only passive stimuli could be simulated by using ‘TouchSim’.

Therefore, the *in-vivo* discrimination test based on passive stimuli was also conducted under the instruction of [41]. The discrimination accuracy achieved by 'TouchSim' was then compared with the multi-level numerical model under passive stimuli together with the *in-vivo* experimental results in this study.

III. RESULTS

A. Predicted tactile signals of the single afferent neural fiber

The stress/strain related quantities including maximum principal strain/stress, vertical strain etc. were correlated with the results of microneurography and the quantity achieving the best fit with the experimental results was selected to be the input of the membrane current transduction model. The stimulation onto the fingertip during microneurography was simulated by using the FE hand model. The strain energy density and other stress/strain related mechanical quantities were obtained under the stimulating force of 2N for the receptive field of SAI and FAI unit. The spatial profiles of strain energy density, maximum principal stress/strain and vertical stress were compared with the microneurography results in Fig. S2. A linear relationship between the neural action potential level and mechanical quantities was assumed in the form of:

$$N_i = aS_i + b \ldots\ldots\ldots\ldots\ldots\ldots\ldots \quad (14)$$

Where N_i is the neural activation potential level and S_i stands for the simulated results. The constants a and b were derived by maximizing the FSS (equation 10) between the microneurography data and the predicted mechanical quantities.

The FSS value of 1 means a perfect match between predictions and experiment results. Predictions were made based on twelve different stress/strain related quantities (see Table. S1) and it was found that strain energy density can provide the best fit with the FSS values of 0.92 and 0.69 for SAI and FAI unit, respectively. This conclusion is in agreement with other researchers [22]. Therefore, the strain energy density was used to correlate the skin mechanics with neural activity for this research.

The original and optimized parameters of the transduction and Izhikevich neural dynamic model were presented in Table S2 and S3. Four and six iterations of RSM were performed for SAI and FAI unit respectively, resulting in the FSS values of 0.9377 and 0.8235.

The neural action potential level under the stimulating force of 2.4N for SAI and FAI unit are used as out-of-sample validation (see Fig. 6). The predicted and experimental spiking rates are close to each other for both SAI and FAI units. For the SAI unit, the predicted results got a wider range of variation than the experimental results. The FAI unit only responded to the 'onset' and 'offset' of the stimulation during the microneurography test while for the predicted results, the FAI unit still fired a few spikes at the lower frequencies.

B. Predicted tactile signals of the population-level afferent neural fiber and its validation

The predicted spiking rates and first spike latency in terms of the population-level afferent tactile units over the finger pad were plotted and visualized in Figure 7. The comparison between the predicted discrimination accuracy and the *in-vivo* psychophysical experimental results is presented in Figure 8 and 9. The active touch is divided into two stages including the dynamic ramp-up of the contact force and static hold of the finger.

It can be seen from Figure 8, the predicted discrimination accuracy agreed well with the experimental results. the convex with the curvature of RC8503, RC532, RC179, RC106, RC77.7, RC48.9mm were numbered from convex 1 to 6. The hit rates are all increased with the curvature of the convex surfaces with regard to the first spike latency and the two stages of the active touch. In the case of the SAI unit, the predicted accuracies are larger than those of the human subject for discriminating the smaller curvatures (convex surface of RC8503, RC532mm differentiated from the flat plate). Whereas the curvature increases, the predicted accuracies are lower than the subject's (hit rate was close to 100%) for the convex surface of RC77.7 and RC48.9mm. The predicted accuracy during the static hold is closer to experimental results than those in terms of the first spike latency and dynamic ramp-up. The standard deviations for the predicted and experimental results decrease with the curvature of the convex.

Figure 9 shows the predictive accuracy and experimental results for the FAI unit. The static hold is not included since the FAI unit mainly responds to the dynamic stimulation. In contrast to the SAI unit, the most accurate prediction was achieved based on the first spike latency. For the procedure of 'Dynamic ramp-up', the predicted accuracies for discriminating convex surface with a small radius are larger than the experimental results, while in the case of discriminating convex surface with a larger radius the predicted accuracies were smaller than the experimental results. This is similar to the SAI unit. The standard deviations for predicted and experimental results are all decreased with the radius of the stimulator. The discrimination accuracy predicted based on the uniformly distributed receptive field of cutaneous neurons was compared with that of heterogeneous one (See Fig. S3 and S4). The results suggested that most of the discrimination accuracy computed based on the tactile units with heterogeneous receptive fields achieved a better agreement with the human subject than the predicted results based on the uniformly distributed receptive fields.

The discrimination accuracy achieved based on the predicted afferent tactile signals through 'TouchSim' [8] was compared with that using the multi-level numerical model (See Fig. S5 and S6). The results showed that the predicted neural signals through 'TouchSim' are consistent with those based on the multi-level numerical model while the predicted discrimination accuracy of 'TouchSim' is slightly closer to the human subject than that of the multi-level numerical model. However, these afferent tactile signals were computed under the condition of passive stimuli, the skin mechanics under active touch is not accessible through 'TouchSim' [8]. Therefore, the multi-level model developed in this research achieved comparable performance with 'TouchSim' on predicting the afferent tactile signals under passive stimuli but with a further capability to obtain the cutaneous neural response evoked during active touch.

IV. Discussion

In this study an integrated numerical model was developed and validated for SAI and FAI afferent, combining the skin mechanics and neural dynamics to predict the single and population-level response of the 1st order cutaneous neurons. The model development was carried out on three levels: (A) on the skin mechanics level by using a subject-specific FE human hand model, (B) validation of the signals from single afferent fiber with the FSS of 0.94 and 0.82 for SAI and FAI unit respectively compared to the microneurography results, (C) the discrimination accuracies of two tactile units achieved the good agreement with the *in-vivo* discrimination test results. The model of population-level neural tactile SAI and FAI unit can differentiate the convex surface with RC8503mm from a flat plate.

The FE human hand served as the skin mechanics model so that the muscle forces and kinematics of active touch can be incorporated. The transduction mechanism between the afferent neural signal and neural activation level of the muscle synergy during active touch can also be investigated. Therefore, this integrated numerical model provides the possibility and push a further step to the explicit studying of sensorimotor mechanism compared with previous studies [9, 22, 45]. The realistic contact mechanism and anatomically intact human hand model provide the actual skin mechanics for predicting neural signals, rather than using the simplified continuum model or regression algorithm [8, 41, 46]. Also, this integrated model can help to predict reliable afferent cutaneous neural signals without the need to carry out microneurography or microsimulation as done previously [15-17, 47]. The subject-specific microneurography and *in-vivo* psychophysical experimental data with an integrated numerical model were employed to study the tactile neural coding and human perception. The predicted population-level 1st order neural signals under active tactile exploration suggest that different coding mechanisms might be applied for the afferent tactile signals elicited from different mechanoreceptors simultaneously.

Microneurography was performed on the subject of the FE hand model. Approximately 75% of the test results were applied for the optimization of the transduction and Izhikevich neural dynamic model, the other 25% of data was used for validation against the predicted results. For the validation of an SAI tactile unit the predicted firing rates varied more greatly than the experimental results, this may be due to the hyperplastic material properties defined for soft tissues in the FE model. The stress is sensitive to the strain variation resulting in large variations of SED and membrane current. In the case of the FAI unit, the predicted firing rates agreed well with the microneurography results during the 'onset' and 'offset', achieving the FSS of 0.82 for all the data points. However, when the RTS was sweeping over the receptive area of the FAI unit, the receptors gave no response with the neural action potential level of 0 spikes/second while the predicted spiking rate was maintained at approximately 20 spikes/second. It can be found from the neural dynamic model for the FAI unit (see equation 4), the firing rate depends on the derivative of the membrane current on the time domain. The SED varied slightly when the stimulator was sweeping over FE hand while this variation may initiate the drifting of the predicted membrane current.

The probabilistic psychophysical prediction was made by using the Gradient Sum method. The spiking rate or the first spike latency was transferred element by element throughout the population. Therefore, each convexity can be represented as a single number as the gradient sum. Here, the population responses during active touch were obtained and compared with the subject-specific discrimination results. The predicted discrimination results for both SAI and FAI units agreed well with the experimental results. During the *in-vivo* discrimination test, the convex surfaces with a small curvature like RC48.9mm is easy to be discriminated from flat plate for the human subject (from the subject's personal feeling). Therefore, the experimental discrimination accuracies of population-level SAI and FAI units are smaller than the predicted ones for discriminating convex surfaces with small curvatures while in case of discriminating the convex surface with a large radius, the subject's success rate became smaller than the simulated results. This might be affected by the subject's human factor since a large number of comparisons need to be completed through the experiment. The two stages of active touch and the first spike latency are good candidates to make the prediction based on this multi-physics model. However, the static hold can provide the best fit for the human discrimination test results which means the perception may rely on rate coding for the signals from SAI units. Unlike the SAI units, perception may depend on the temporal coding of FAI afferents since the predicted accuracy based on first spike latency achieved the best agreement with the experimental results. These findings support the assumptions made by other researchers [48, 49] that humans may use multiple coding strategies simultaneously. The temporal coding may be used for fast identification of a stimulus and triggering the reactions while rate coding can represent the quantities of the stimulus. The similar perception was evoked based on the neural information conveyed by these two tactile afferents but relying on two different coding mechanisms, suggesting that different types of tactile neurons could be independent in haptic systems. The noise applied to the firing rates and first spike latency can affect the predicted accuracy, the effect was shown in Fig. S7. The simulation results have shown that the complex and heterogeneous distributed receptive filed of cutaneous neurons help to enhance the discrimination accuracy compared with those under the uniform distribution. These larger and more complex overlapped receptive fields with multiple ‘hotpots’ or sensitive zones enable a higher spatial resolution which echoes the finding of other researchers [25]. However, the afferent branching mechanism through which the end organs of the cutaneous receptors are integrated to elicit the afferent neural signals is still unclear so far [29, 50]. More simulations on active touch could be conducted to study the effects of these heterogeneous receptive fields on human tactile performance after gaining a solid understanding of the branching mechanism of cutaneous receptors.

The discrimination accuracy archived based on the cutaneous neural responses predicted through this multi-level model was compared with that of ‘TouchSim’ [8]. ‘TouchSim’ achieved a more human-like tactile performance than the multi-level numerical model based on the passive external stimuli. Despite the high computing efficiency and better performance of ‘TouchSim’ under passive stimuli [8], the multilevel numerical model developed in this study takes the 3D geometry of the human hand and the muscle-driven active touch into consideration while maintaining a comparable performance on predicting the afferent tactile signals with ‘TouchSim’.

This validated multi-level numerical model provides the possibility for pioneering research on human tactile sensing under the active touch and sensorimotor mechanism. For example, the relationship between population-level afferent signals and the neural activation level of muscle synergy could be explicitly summarized and applied to the control of bionic or prosthetic hand to restore the performance of the human hand [51, 52]. However, the FE human hand model was involved in this numerical tool, resulting in the high computational cost. The surrogate modelling based on this FE model needs to be developed to reduce the computational cost and make it user-friendly to other researchers. Also, this multi-level numerical model can only predict the neural response of two type I tactile units. The convergence of the 1st order tactile signals from the ulna and median nerve and their post-processing were not included in this research. Future work can focus on simulating the responses of the two type II mechanoreceptors and the convergent mechanism of the population-level cutaneous neural signals transferred along different nerves.

V. Conclusion

The FE human hand model was combined with mechanoelectrical transduction and neural dynamic model for predicting afferent tactile neural signals during active tactile exploration. The relationship between external stimuli and cutaneous neural activities was computed based on subject-specific microneurography data, approximately 75% of the test results was applied for the model optimization and another 25% was used for validation. Human perception during an active discriminating test was correlated with the population-level tactile neural signals achieving similar tactile discrimination abilities to the human subject. The predicted cutaneous neural signals under active touch suggest that human perception during active touch exploration may simultaneously rely on different coding mechanisms for the neural signals elicited from different classes of cutaneous receptors. It was found that the heterogeneously distributed receptive fields may help to achieve a better sensing performance than the uniformly distributed ones. Comparable discrimination accuracies are observed between this multi-level numerical model and the published benchmark model [8], while the former presents the further capability of predicting the afferent neural response under the active touch. The 3D geometry of the finger pad and hand kinematics are also involved. This integrated numerical model provides a new concept to effectively study the human tactile seeing and sensorimotor mechanism under the active touch.

Acknowlegement

This research was partly supported by the National Key Research and Development Program of China (grant 2018YFC2001300), the National Natural Science Foundation of China (grants 91948302, 91848204, and 52021003).

Conflict of interest

The authors declare that they have no conflicts of interest.

References

[1] E. R. Kandel *et al.*, *Principles of neural science*. McGraw-hill New York, 2000.

[2] G. Valle *et al.*, "Biomimetic Intraneural Sensory Feedback Enhances Sensation Naturalness, Tactile Sensitivity, and Manual Dexterity in a Bidirectional Prosthesis," *Neuron,* vol. 100, no. 1, pp. 37-45 e7, Oct 10 2018, doi: 10.1016/j.neuron.2018.08.033.

[3] K. O. Johnson, "Neural coding," *Neuron,* vol. 26, no. 3, pp. 563-566, 2000.

[4] B. M. Calancie and R. Stein, "Microneurography for the recording and selective stimulation of afferents: An assessment," *Muscle & Nerve: Official Journal of the American Association of Electrodiagnostic Medicine,* vol. 11, no. 6, pp. 638-644, 1988.

[5] A. B. Vallbo, K.-E. Hagbarth, and B. G. Wallin, "Microneurography: how the technique developed and its role in the investigation of the sympathetic nervous system," *Journal of Applied Physiology,* vol. 96, no. 4, pp. 1262-1269, 2004.

[6] K. Dandekar, B. I. Raju, and M. A. Srinivasan, "3-D finite-element models of human and monkey fingertips to investigate the mechanics of tactile sense," *Journal of biomechanical engineering,* vol. 125, no. 5, pp. 682-691, 2003.

[7] G. J. Gerling, Rivest, II, D. R. Lesniak, J. R. Scanlon, and L. Wan, "Validating a population model of tactile mechanotransduction of slowly

adapting type I afferents at levels of skin mechanics, single-unit response and psychophysics," *IEEE Trans Haptics,* vol. 7, no. 2, pp. 216-28, Apr-Jun 2014, doi: 10.1109/TOH.2013.36.

[8] H. P. Saal, B. P. Delhaye, B. C. Rayhaun, and S. J. Bensmaia, "Simulating tactile signals from the whole hand with millisecond precision," *Proceedings of the National Academy of Sciences,* vol. 114, no. 28, pp. E5693-E5702, 2017.

[9] D. R. Lesniak and G. J. Gerling, "Predicting SA-I mechanoreceptor spike times with a skin-neuron model," *Math Biosci,* vol. 220, no. 1, pp. 15-23, Jul 2009, doi: 10.1016/j.mbs.2009.03.007.

[10] C. Xu, Y. Wang, and G. J. Gerling, "Individual Performance in Compliance Discrimination is Constrained by Skin Mechanics but Improved under Active Control," in *2021 IEEE World Haptics Conference (WHC)*, 2021: IEEE, pp. 445-450.

[11] C. Simões-Franklin, T. A. Whitaker, and F. N. Newell, "Active and passive touch differentially activate somatosensory cortex in texture perception," *Human brain mapping,* vol. 32, no. 7, pp. 1067-1080, 2011.

[12] A. M. Smith, C. E. Chapman, F. Donati, P. Fortier-Poisson, and V. Hayward, "Perception of simulated local shapes using active and passive touch," *Journal of neurophysiology,* vol. 102, no. 6, pp. 3519-3529, 2009.

[13] R. Grant, P. M. Itskov, B. Towal, and T. J. Prescott, "Active touch sensing: finger tips, whiskers, and antennae," *Frontiers in behavioral neuroscience,* vol. 8, p. 50, 2014.

[14] R. S. Johansson and J. R. Flanagan, "Coding and use of tactile signals from the fingertips in object manipulation tasks," *Nature Reviews Neuroscience,* vol. 10, no. 5, pp. 345-359, 2009.

[15] J. Ochoa and E. Torebjörk, "Sensations evoked by intraneural microstimulation of single mechanoreceptor units innervating the human hand," *The Journal of physiology,* vol. 342, no. 1, pp. 633-654, 1983.

[16] R. Romo, "Hernandez A, Zainos A, and Salinas E," *Somatosensory discrimination based on cortical microstimulation. Nature,* vol. 392, pp. 387-390, 1998.

[17] S. N. Flesher *et al.*, "Intracortical microstimulation of human somatosensory cortex," *Science translational medicine,* vol. 8, no. 361, pp. 361ra141-361ra141, 2016.

[18] B. Lee *et al.*, "Engineering artificial somatosensation through cortical stimulation in humans," *Frontiers in systems neuroscience,* vol. 12, p. 24, 2018.

[19] Y. Wei, Z. Zou, G. Wei, L. Ren, and Z. Qian, "Subject-specific finite element modelling of the human hand complex: muscle-driven simulations and experimental validation," *Annals of Biomedical Engineering,* pp. 1-15, 2019.

[20] G. Harih, R. Nohara, and M. Tada, "Finite Element Digital Human Hand Model-Case Study of Grasping a Cylindrical Handle," *Journal of Ergonomics,* vol. 07, no. 02, 2017, doi: 10.4172/2165-7556.1000190.

[21] J. R. Holt and D. P. Corey, "Two mechanisms for transducer adaptation in vertebrate hair cells," *Proceedings of the National Academy of Sciences,* vol. 97, no. 22, pp. 11730-11735, 2000.

[22] T. Q. Pham, T. Hoshi, Y. Tanaka, and A. Sano, "Effect of 3D microstructure of dermal papillae on SED concentration at a mechanoreceptor location," *PloS one,* vol. 12, no. 12, p. e0189293, 2017.

[23] J. A. Pruszynski and R. S. Johansson, "Edge-orientation processing in first-order tactile neurons," *Nature neuroscience,* vol. 17, no. 10, pp. 1404-1409, 2014.

[24] R. S. Johansson, "Tactile sensibility in the human hand: receptive field characteristics of mechanoreceptive units in the glabrous skin area," *The Journal of physiology,* vol. 281, no. 1, pp. 101-125, 1978.

[25] E. Jarocka, J. A. Pruszynski, and R. S. Johansson, "Human touch receptors are sensitive to spatial details on the scale of single fingerprint ridges," *Journal of Neuroscience,* vol. 41, no. 16, pp. 3622-3634, 2021.

[26] N. Cauna, "Nerve supply and nerve endings in Meissner's corpuscles," *American Journal of Anatomy,* vol. 99, no. 2, pp. 315-350, 1956.

[27] N. Cauna, "The mode of termination of the sensory nerves and its significance," *Journal of Comparative Neurology,* vol. 113, no. 2, pp. 169-209, 1959.

[28] M. Nolano *et al.*, "Quantification of myelinated endings and mechanoreceptors in human digital skin," *Annals of neurology,* vol. 54, no. 2, pp. 197-205, 2003.

[29] M. Paré, A. M. Smith, and F. L. Rice, "Distribution and terminal arborizations of cutaneous mechanoreceptors in the glabrous finger pads of the monkey," *Journal of Comparative Neurology,* vol. 445, no. 4, pp. 347-359, 2002.

[30] R. S. Johansson and A. B. Vallbo, "Tactile sensibility in the human hand: relative and absolute densities of four types of mechanoreceptive units in glabrous skin," *The Journal of physiology,* vol. 286, no. 1, pp. 283-300, 1979.

[31] D. Quintero, "Properties of cutaneous mechanoreceptors in the human hand-related to touch sensation," 1984.

[32] E. M. Izhikevich, "Simple model of spiking neurons," *IEEE Transactions on neural networks,* vol. 14, no. 6, pp. 1569-1572, 2003.

[33] A. Chami, M. Ohka, Y. Kawabe, and H. B. Yussof, "Response of SAI Afferents May Play a

Role in the Perception of Velvet Hand Illusion 1," 2010.

[34] M. Condon *et al.*, "Differential sensitivity to surface compliance by tactile afferents in the human finger pad," *Journal of Neurophysiology,* vol. 111, no. 6, pp. 1308-1317, 2014.

[35] S. B. Park *et al.*, "Fast-adapting mechanoreceptors are important for force control in precision grip but not for sensorimotor memory," *Journal of neurophysiology,* vol. 115, no. 6, pp. 3156-3161, 2016.

[36] R. S. Johansson and Å. B. Vallbo, "Tactile sensory coding in the glabrous skin of the human hand," *Trends in neurosciences,* vol. 6, pp. 27-32, 1983.

[37] R. G. Hallin, "Microneurography in relation to intraneural topography: somatotopic organisation of median nerve fascicles in humans," *Journal of Neurology, Neurosurgery & Psychiatry,* vol. 53, no. 9, pp. 736-744, 1990.

[38] N. D. Strzalkowski, R. M. Peters, J. T. Inglis, and L. R. Bent, "Cutaneous afferent innervation of the human foot sole: what can we learn from single-unit recordings?," *Journal of neurophysiology,* vol. 120, no. 3, pp. 1233-1246, 2018.

[39] N. Salimi-Nezhad, M. Amiri, E. Falotico, and C. Laschi, "A Digital Hardware Realization for Spiking Model of Cutaneous Mechanoreceptor," *Frontiers in Neuroscience*, vol. 12, 2018.

[40] H. Stanislaw and N. Todorov, "Calculation of signal detection theory measures," *Behavior research methods, instruments, & computers,* vol. 31, no. 1, pp. 137-149, 1999.

[41] A. Goodwin, K. John, and A. Marceglia, "Tactile discrimination of curvature by humans using only cutaneous information from the fingerpads," *Experimental brain research,* vol. 86, no. 3, pp. 663-672, 1991.

[42] F. D. Farfan, J. C. Politti, and C. J. Felice, "Evaluation of EMG processing techniques using Information Theory," *Biomed Eng Online,* vol. 9, p. 72, Nov 12 2010, doi: 10.1186/1475-925X-9-72.

[43] C. J. De Luca, L. D. Gilmore, M. Kuznetsov, and S. H. Roy, "Filtering the surface EMG signal: Movement artifact and baseline noise contamination," *J Biomech,* vol. 43, no. 8, pp. 1573-9, May 28 2010, doi: 10.1016/j.jbiomech.2010.01.027.

[44] T. Butler, S. Kilbreath, R. Gorman, and S. Gandevia, "Selective recruitment of single motor units in human flexor digitorum superficialis muscle during flexion of individual fingers," *The Journal of physiology,* vol. 567, no. 1, pp. 301-309, 2005.

[45] F. Crevecoeur, A. Barrea, X. Libouton, J. L. Thonnard, and P. Lefevre, "Multisensory components of rapid motor responses to fingertip loading," *J Neurophysiol,* vol. 118, no. 1, pp. 331-343, Jul 1 2017, doi: 10.1152/jn.00091.2017.

[46] R. S. Johansson and I. Birznieks, "First spikes in ensembles of human tactile afferents code complex spatial fingertip events," *Nature neuroscience,* vol. 7, no. 2, p. 170, 2004.

[47] L. Johnson, J. Wander, D. Sarma, D. Su, E. Fetz, and J. Ojemann, "Direct electrical stimulation of the somatosensory cortex in humans using electrocorticography electrodes: a qualitative and quantitative report," *Journal of Neural Engineering,* vol. 10, no. 3, p. 036021, 2013.

[48] M. Bieler, K. Sieben, N. Cichon, S. Schildt, B. Röder, and I. L. Hanganu-Opatz, "Rate and temporal coding convey multisensory information in primary sensory cortices," *eneuro,* vol. 4, no. 2, 2017.

[49] S. Terada, Y. Sakurai, H. Nakahara, and S. Fujisawa, "Temporal and rate coding for discrete event sequences in the hippocampus," *Neuron,* vol. 94, no. 6, pp. 1248-1262. e4, 2017.

[50] E. D. Kuehn, S. Meltzer, V. E. Abraira, C.-Y. Ho, and D. D. Ginty, "Tiling and somatotopic alignment of mammalian low-threshold mechanoreceptors," *Proceedings of the National Academy of Sciences*, vol. 116, no. 19, pp. 9168-9177, 2019.

[51] Y. Kim *et al.*, "A bioinspired flexible organic artificial afferent nerve," *Science,* vol. 360, no. 6392, pp. 998-1003, 2018.

[52] J. J. Cone, A. M. Ni, K. Ghose, and J. H. Maunsell, "Electrical microstimulation of visual cerebral cortex elevates psychophysical detection thresholds," *Eneuro,* vol. 5, no. 5, 2018.